

LOW-TEMPERATURE HYDROTHERMAL ALTERATION IN NEAR-SURFACE
SEDIMENTS, SALTON SEA GEOTHERMAL AREA

Anne Sturz

Scripps Institution of Oceanography, Geological Research Division,
University of California, San Diego, La Jolla, California

Abstract. As part of the Lawrence Livermore/Sandia National Laboratories shallow drilling (19 wells) into Salton Sea sediments, four 1-m cores were recovered from 76 m subbottom depth. The cored wells are along a transect from the margin toward the interior of the Mullet Island thermal anomaly. The thermal gradients range from 0.191°C/m near the margin to 0.816°C/m near the interior of the thermal anomaly. Bottom-hole temperature in a cored well close to the center of the thermal anomaly is 87°C. Pore water chemical composition and bulk and clay size sediment mineralogical and chemical compositions are influenced by hydrothermal reactions which intensify with increasing thermal gradient. X ray diffraction and petrographic microscopic analyses of bulk and clay size fractions of the sediments indicate that the relative proportions of smectite to kaolinite plus illite and of dolomite to calcite increase from the margin toward the interior of the thermal anomaly region. Clay mineral recrystallization and dolomitization are indicated by increased K/Al and decreased Ca/Mg molar ratios in the clay size sediment fraction. Calcium, silica, potassium, lithium, and strontium are released from sediments into pore fluids. These data suggest that even at temperatures less than 100°C, hydrothermal activity significantly alters the pore water chemistry and moderately alters the sediment mineralogical and chemical composition.

Introduction

The Salton Trough is a sediment-filled rift zone located at the northern end of the Gulf of California (Figure 1), at the transition from extension-dominated tectonics of the East Pacific Rise to transform-dominated tectonics of the San Andreas fault system. Within the Salton Trough, the Salton Sea Geothermal Area is among several well-documented sites of hydrothermal activity associated with magma intrusion into the sediment blanket [e.g., Randall, 1974; Elders, 1984; Younker et al., 1982; Newmark et al., 1986].

Hydrothermally driven reactions between pore fluids and sediments influence the mineralogical composition of the sediments and the chemical compositions of the sediments, the pore fluids, and the overlying water column. Such reactions which occur in the sediments adjacent to the magmatic intrusion have resulted in sediment alteration to the greenschist facies and the formation of base metals enriched pore fluids [Skinner et al., 1967; Rex, 1983; Elders, 1984]. Near-surface sediments are insulated from the

extreme temperatures and chemical perturbations associated with magmatic activity at depth by interjacent impermeable sediments. In spite of less intense alteration, hydrothermally driven reactions between near-surface sediments and pore fluids may be geochemically significant.

Hydrothermal systems at sediment-blanketed rise crests are thought to be sites of active base metal deposition [Von Damm et al., 1985]. The Salton Sea Geothermal Area is known to have very high concentrations of base metals in the deep reservoir brine [Helgeson, 1968; Elders, 1984]. One of the main objectives of this study was to search for unique geochemical signatures, acquired and retained in near-surface hydrothermally altered sediments at moderate temperatures, in a system with active ore deposition at depth. If identified, they might be applied to geochemical exploration for sites of extinct ore deposition in tectonically similar regions.

Salton Trough sediments include interlayered shales, evaporites, siltstones, well-sorted sandstones, and gravel deposits. They accumulated primarily as alluvial fans, lacustrine, and Colorado River deltaic deposits [Muffler and Doe, 1968; Muffler and White, 1969; Randall, 1974]. The varied depositional environments in which these sediments accumulated impose a heterogeneous distribution of primary permeability. Generally in this area, transitional terrestrial-shallow marine sediments underlie lacustrine sediments. The transitional terrestrial-shallow marine units are dominated by more permeable fluvial-deltaic siltstones, sandstones, and gravels deposited in the Gulf of California. The lacustrine units are dominated by less permeable evaporites, poorly consolidated muds, and shales deposited in the Salton Trough after it was isolated from the Gulf of California in the mid-Pleistocene [Randall, 1974]. Thus the overall permeability structure has been divided into two sections, an impermeable upper cap overlying a more permeable reservoir sequence. Based on geophysical well logs and petrology of well cores and cuttings, Randall [1974] interprets this permeability distribution to be original, a depositional permeability distribution.

The present-day distribution of heat transfer processes within the sediments, which is controlled primarily by sediment permeability, shows a typical profile that is composed of two parts [Younker et al., 1982]. In the upper cap the vertical heat transfer process is dominated by steady state conduction. In the lower, more permeable reservoir, heat transfer is by convection. Based on well log geophysical data and the distribution of the two-part heat transfer profiles, Younker et al. [1982] defined the lower boundary of a thermal cap which does

Copyright 1989 by the American Geophysical Union.

Paper number 88JB04271.
0148-0227/89/88JB-04271\$05.00

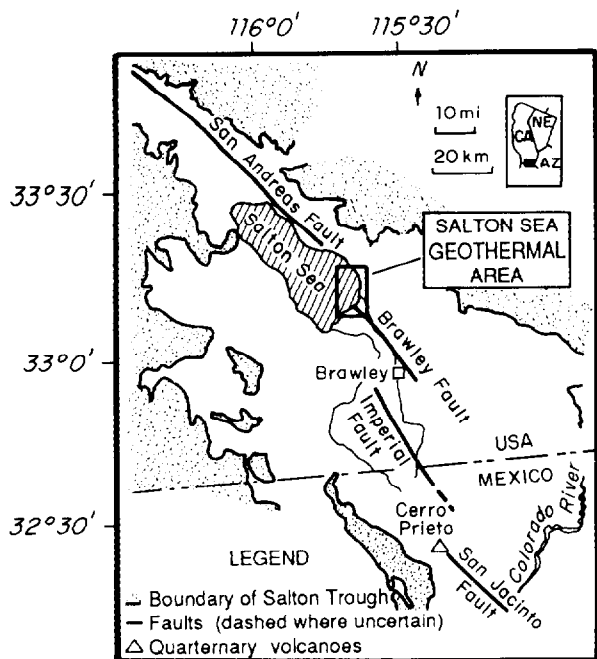


Fig. 1. Generalized location map of the Salton Sea Geothermal Area [Newmark et al., 1986].

not coincide with the lower boundary of the lithologic cap of Randall [1974]. This thermal cap is considered to have formed by permeability reduction superimposed on the original depositional permeability, in response to precipitation of pore-filling hydrothermal minerals. In the interpretation of Younker et al. [1982], the boundary between overlying impermeable cap and the underlying permeable reservoir sediments is delineated by a thermal-chemical front along which rocks have been sealed by hydrothermal mineral precipitation.

One could distinguish between the lithologic cap and thermal cap interpretations by examining, in the shallowest part of the cap unit, the horizontal distributions of variations in major and trace element chemical composition of pore fluids and authigenic minerals along a transect across the thermal anomaly. Specifically, one could look for evidence of shallow hydrothermal alteration in near-surface cap sediments overlying the deep-seated thermal anomaly and for evidence of chemical exchange between near-surface sediments and the deep-seated thermal reservoir fluid. The geochemical signatures acquired and retained in pore fluids and authigenic solids formed in such different environments are expected to be different.

The reservoir fluid within the Salton Sea Geothermal Area has a unique geochemical composition which can be used to trace its presence. This fluid is a base metals enriched (e.g., copper, zinc, lead, nickel, chromium, and silver) chloride brine [e.g., Skinner et al., 1967; Helgeson, 1968; Rex, 1983; Elders, 1984]. Based on strontium and lead isotopic evidence, the source of these two and most likely also the other dissolved metals in the Salton Sea geothermal brine is considered to be the reservoir host sediment [Skinner et al., 1967; Muffler and Doe, 1968]. Brine types in the

Imperial Valley were classified by Rex [1983] on the basis of Cl^-/Br^- ratios. Cl^-/Br^- might be a useful tracer of water provenance because this ratio is assumed to be unaffected by metamorphic processes. The deep reservoir brine, derived primarily from halide dissolution as cold groundwater encounters evaporites, was subsequently altered by hydrothermal reactions with the sediments adjacent to the thermal reservoir. As heated fluids equilibrated with the host sediments, metals were leached and retained as dissolved complexes. The deep-seated reservoir brine Cl^-/Br^- ratio is greater than 20,000 (concentration ratio). Modern Salton Sea water has a significantly lower Cl^-/Br^- ratio, of 290, and is poor in dissolved metals relative to the reservoir brine. Therefore, if the near-surface sediments, with pore water originally derived from the Salton Sea, would be affected by relatively low-temperature hydrothermal reactions only, the original pore water chemistry would be still easily recognized and should also be reflected in the authigenic minerals. The resulting fluid would not show the high Cl^-/Br^- ratio and metals concentrations observed in the high-temperature deep-seated brine. If, however, the near-surface sediments would be affected by a hydrothermal front derived from the deep-seated reservoir brine, the pore fluid chemical composition and the authigenic mineralogy and chemistry would acquire and retain relatively high concentrations of base metals and a high Cl^-/Br^- ratio.

In the present study I searched for geochemical and mineralogical evidence for hydrothermal interaction between surface sediments overlying the Salton Sea Geothermal Area and the geothermal reservoir brine at depth. I looked for geochemical indications, such as anomalies in Salton Sea sediments, which could be used to distinguish between two types of hydrothermally altered sediments: (1) those influenced by alteration reaction at elevated temperatures with their original pore fluid but not with the underlying hydrothermal reservoir brine and (2) those influenced by both the thermal anomaly and by chemical reactions with the underlying geothermal brine.

In order to distinguish between these two types of altered sediments and to distinguish between the lithologic and thermal cap interpretations, the original, unaltered sediment mineralogical and chemical composition needs to be considered as well.

The data presented here, from four 1-m-long Salton Sea sediment cores recovered from the bottom of each of the wells at 76 m subbottom depth, include chemical analyses of pore fluids and chemical and mineralogical analyses of bulk sediment and of the clay size sediment fraction.

These cores transect the Mullet Island thermal anomaly, from the northwesterly margin toward the center (Figure 2) [Newmark et al., 1988]. Bottom-hole temperatures in the four cored shallow wells range from 37°C to 90°C. The thermal gradient ranges from 0.191°C/m to 0.816°C/m [Newmark et al., 1988].

In November-December 1985, 19 wells were drilled into Salton Sea sediments by Lawrence Livermore/Sandia National laboratories [Newmark et al., 1986, 1988]. Cuttings were recovered at 3-m intervals from all 19 wells. Cores of 1-m

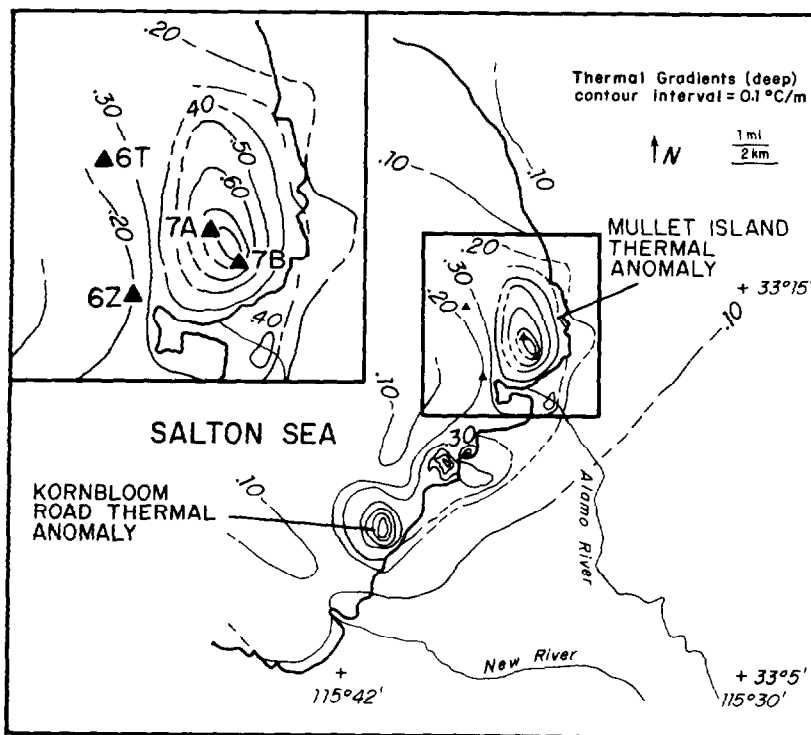


Fig. 2. Thermal gradients, Salton Sea Geothermal Area, with 0.1°C/m contour intervals and location of wells 7B, 7A, 6T, and 6Z [after Newmark et. al, 1988].

length were recovered from the 76-m depth interval from each of four wells. One of the main objectives of this program was to complete the surficial coverage of thermal measurements needed to define the shape and lateral extent of the Salton Sea Geothermal Area thermal anomaly. The shape of the Axial thermal anomaly is arcuate and asymmetric with respect to a line of volcanoes previously thought to represent the center of the field. Heat flow in the central part of the field is greater than 600 mW/m². In

the area of this study, thermal gradients rise across a narrow (2.4 km) zone from the regional thermal gradient of 0.09-0.85°C/m. Areas of high thermal gradient (above 0.8°C/m) center about Mullet Island and to the southwest near Kornbloom Road (Figure 2).

Experimental Methods

Pore water was extracted from each of the four cores by centrifugation within 4 hours of core

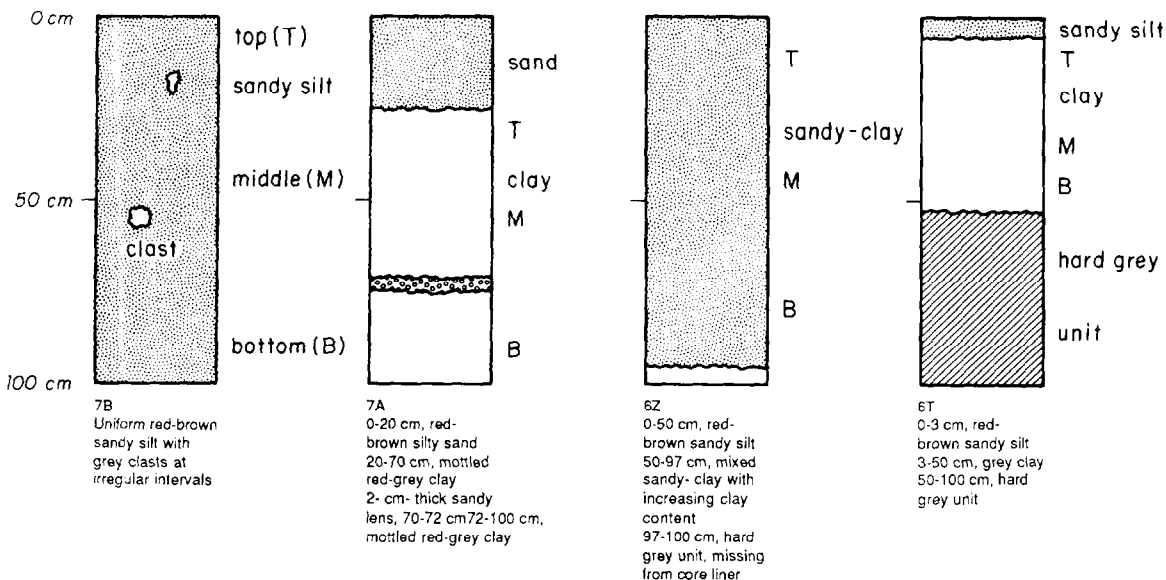


Fig. 3. Schematic core diagrams with subsample locations. T, top; M, middle; B, bottom.

TABLE 1. Chemical Composition of Pore Waters

	Site				Salton Sea Water	Percent Error	Salton Sea Deep Reservoir Brines*
	7B	7A	6Z	6T			
Temperature Gradient, °C	0.8	NL	0.2	0.2			
Bottom-Hole Temperature, °C	87	90	37	40			
Alk, meg/l	7.3	3.2	3.3	5.5	4.2	1	
pH (25°C)	6.8	7.5	7.7	8.0	8.4	1	
Ca, mmol	50.2	42.0	39.7	31.3	24.5	1	719
Mg, mmol	44.7	55.7	61.7	58.6	50.9	1	0.4
Ca/Mg	1.13	0.75	0.64	0.54	0.48		1,798
Si, µmol	317	70	96	96	120	1	14
Chlorinity, mmol	762	759	627	622	450	1	43,722
K, mmol	22.1	7.8	6.3	5.3	6.4	3	423
Li, mmol	4.4	3.2	1.6	1.0	0.6	2	30
Sr, mmol	0.76	0.74	0.49	0.22	0.27	2	5
Cl ⁻ /Br ⁻	370	NA	NA	376	290		>20,000**
Cu, ppm	0.11	0.07	0.07	0.07	0.07	1	3
Zn, ppm	0.13	0.11	0.06	0.06	0.01	3	500
Ni, ppm	0.2	0.2	0.2	0.2	0.2	1	
Cr, ppm	0.19	0.19	0.19	0.19	0.08	5	

NL, nonlinear thermal gradient; NA, data not available.

* from Helgeson [1968].

** from Rex [1983].

recovery. It was immediately filtered, using 0.45-µm millipore filters. One aliquot of pore water was acidified to pH <1 with ultra pure (double distilled) 6 N HCl for dissolved metals analyses. The pH at 25°C and alkalinity by Gran titration were determined immediately. Pore waters were analyzed for calcium, magnesium, and total chlorinity (sum of the halogens) by titration; potassium, lithium, strontium, zinc, lead, copper, nickel, and chromium concentrations by atomic absorption spectroscopy; silica by colorimetry [Gieskes, 1976]; bromide and chloride ions by ion selective Beckman electrode.

Chemical analyses were performed on the bulk sediment from three intervals within each core and in well 7B from five shallower depth intervals using cuttings (Figure 3). Sediment subsamples were washed with double deionized water to remove pore water salts and were air dried prior to preparation for chemical analyses. Bulk mineralogy of solids was determined by petrographic microscopy and X ray diffraction (using CuKα radiation and a nickel filter). Clay mineralogy, using the less than 2-µm size fraction, was determined by comparing untreated, glycolated, and 525°C heat-treated clay mineral diffraction patterns, using the (001) and (060) reflections. Percent clay size fraction was determined gravimetrically after quantitative removal of the clay size fraction by settling.

For major element chemical analyses, bulk sediment and clay size fractions were dissolved by lithium metaborate-tetraborate fluxed fusion at 1000°C, followed by dissolution in 1 N H₂SO₄ [Brown, 1988]. Solutions for trace and minor element chemical analyses were acquired by leaching the sediments with hydroxylamine/hydrochloric acid/hydrofluoric acid/perchloric acid/aqua regia (T. Shaw, personal communication, 1986). The major and trace element chemical

analyses were performed by standard atomic absorption and colorimetric techniques [Brown, 1988].

Results and Discussion

Pore water chemical compositions are given in Table 1 and Figure 4. Bulk sediment chemical compositions are given in Table 2 and Figure 5. Clay size sediment chemical compositions are given in Table 3 and Figure 6. Location of wells 7B, 7A, 6Z, and 6T are given in Figure 2. Schematic core diagrams with subsample locations are given in Figure 3. Wells 7A and 7B are closest to the heat source, and wells 6Z and 6T are nearest the margin of the Mullet Island thermal anomaly (Figure 2). Wells 7B, 6Z, and 6T exhibit linear heat thermal profiles, indicative of conductive heat transfer [Newmark et al., 1988]. Well 7A exhibits a nonlinear thermal profile, where changes in thermal gradient are apparently not related to changes in dominant lithology. This is considered by Newmark et al. (1988) to indicate nonconductive or non-steady state heat transfer.

Randall [1974] concluded that stratigraphic correlation from well to well, even over short distances of tens to hundreds of meters, is difficult. Normal faulting in response to basin formation and lateral transform offset, associated with the transition from East Pacific Rise to San Andreas fault system tectonics, makes it impossible to assume that the 76-meter interval in these four wells has sampled the same stratigraphic unit. No attempt was made during the shallow thermal gradient project drilling program to correlate stratigraphically between wells.

Pore water and sediment chemical compositions given in Tables 1, 2, and 3 suggest concentration

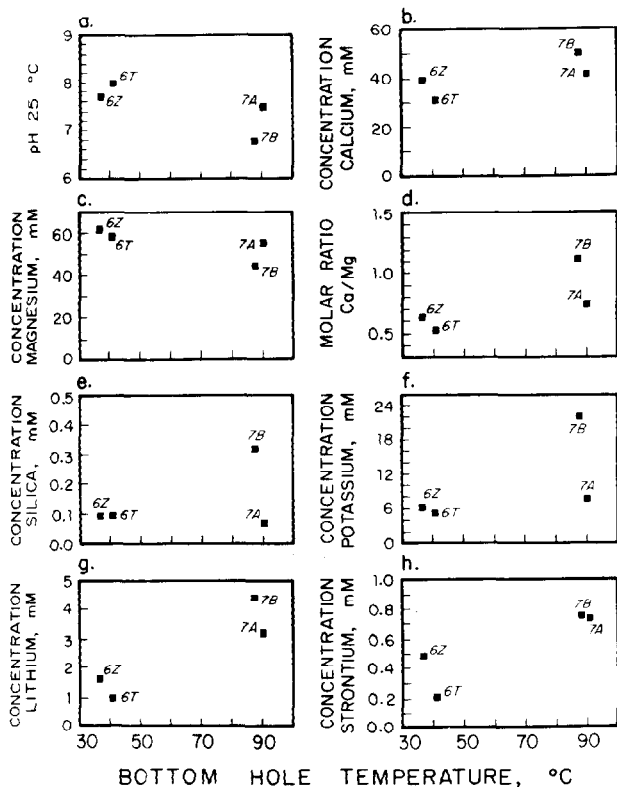


Fig. 4. Pore water composition (in millimoles) versus bottom-hole temperature (in degrees Celsius): (a) pH, (b) calcium, (c) magnesium, (d) Ca/Mg molar ratio, (e) silica, (f) potassium, (g) lithium, (h) strontium.

patterns which can be attributed to hydrothermal activity. The profiles for wells 7B, 6Z, and 6T suggest thermally induced reactions between pore water and solid phases but do not support chemical reactions between these near-surface sediments and the underlying geothermal reservoir deep seated brine.

Pore Water

If one excludes data from well 7A, pore water calcium, silica, chlorinity, potassium, lithium, and strontium concentrations and Ca/Mg molar ratios increase from wells 6T and 6Z, near the margin, toward well 7B in the interior of the thermal anomaly region. Magnesium concentration decreases from wells 6T and 6Z toward well 7B. These data can be interpreted to indicate the release of calcium, silica, potassium, lithium, and strontium into the fluid phase and the removal of magnesium from the fluid phase via thermally accelerated diagenesis reactions between pore water and sediments. Similar trends have been observed as a result of simple diagenesis processes [e.g., Gieskes, 1983]. However, the trends observed in these wells are more pronounced in the higher-temperature well. Therefore these trends may be interpreted as thermally accelerated reactions. The data for pH values and observed Cl^-/Br^- ratios do not require, nor support, chemical reactions with the deep-seated reservoir brine. The Cl^-/Br^- ratio is similar to that of modern Salton Sea water and very different from that of the deep-seated

reservoir brine. The pore waters of these sediments show a trend toward lowered pH with increasing temperature. Decreasing pH with increasing temperature is consistent with trends observed in both natural sedimented-blanketed hydrothermal systems [Von Damm et al., 1985], experimental hydrothermal alteration of basalts [e.g., Bischoff and Dickson, 1975; Bischoff and Seyfried, 1978; Mottl and Seyfried, 1980] and experimental hydrothermal alteration of sediments [Thornton and Seyfried, 1987]. Based on X ray diffraction and smear slide petrographic analyses, dolomite is a minor component (less than 10%) in these sediments. Release of calcium and strontium from calcite and consumption of magnesium during dolomitization and the recrystallization of clay minerals may contribute to the observed trends in calcium, magnesium, and strontium concentrations. Thermally accelerated dolomitization at moderate temperatures resulting in similar calcium, magnesium, and strontium pore water concentration trends has been observed in the Guaymas Basin [Stout and Campbell, 1983; Gieskes et al., 1988]. Recrystallization of clay minerals may be responsible for the observed trends for pH, magnesium, potassium, and silica concentrations in the pore water.

In well 7A, which has the highest bottom-hole temperature, 90°C, pore water concentrations of calcium, magnesium, silica, potassium, and lithium are anomalous when compared to the trends observed in wells 7B, 6T, and 6Z. Concentrations of calcium, silica, potassium, and lithium are lower than expected, and magnesium concentration is relatively high. The anomalous pore water chemical composition found in well 7A may be explained in the light of the nonlinear character of the thermal profile determined in this well by Newmark et al. [1988]. This nonlinear thermal gradient might indicate thermal leakage along a fault in the region of well 7A in an area otherwise dominated by a conductive heat transfer process. In fact, fumaroles have been observed within several meters of the 7A well site. If there is anomalous heat flow and gas discharge, the same path may be used for fluid flow. Unfortunately, Cl^-/Br^- ratio is unavailable for 7A pore water. Without these data, we have insufficient information to verify the source of this fluid. The well 7A pore fluid major element chemical composition, however, suggests shallow lateral fluid flow, rather than mixing with the deep-seated reservoir brine.

Mineralogy

Based on X ray diffraction and smear slide petrographic examination, the major mineralogical components of Salton Sea sediments are detrital quartz, feldspar, and clay minerals, presumably brought into the basin by the Colorado River drainage system. Calcite and dolomite were observed in all four cores. Gypsum is present only in core 6T. The massive nature of the hard, grey, gypsum-bearing unit at the bottom of core 6T implies that this layer is a primary evaporite unit. A hard grey unit was present at the bottom 5 cm of core 6Z. This unit was lost during recovery of the core liner. Small fragments of the 6Z hard grey unit which were stuck to the core barrel were insufficient for petrographic or

TABLE 2. Element/Al Molar Ratios and Trace Element Composition of Bulk Sediments

	7B				7B, Cuttings Depth, m					
	Top	Middle	Bottom	Clast Ash	Surface	0-2	7-9	14-17	45-48	
	Sanday Silt	Sandy Silt	Sandy Silt							
Ca/Mg	0.065	0.059	0.051	0.440	0.571	0.509	0.248	0.298	0.824	
Ca/Al	0.077	0.083	0.081	0.009	0.165	0.135	0.045	0.046	0.034	
Mg/Al	1.186	1.425	1.577	0.019	0.289	0.264	0.180	0.153	0.041	
Na/Al	0.101	0.097	0.099	0.187	0.120	0.079	0.121	0.142	0.061	
K/Al	0.150	0.174	0.185	0.209	0.141	0.125	0.145	0.178	0.141	
Fe/Al	0.139	0.165	0.185	0.132	0.200	0.197	0.175	0.170	0.096	
Ti/Al	0.022	0.025	0.027	0.012	0.028	0.022	0.019	0.017	0.017	
Al, M/kg	2.66	2.30	2.38	2.59	2.20	2.64	3.31	2.59	2.62	
Cu, ppm	29.9									
Zn, ppm	86									
Pb, ppm	< 0.2									
Ni, ppm	< 0.2									
Cr, ppm	72									
Mn, ppm	208									
Li, ppm	58									

	7A				6Z			6T			Grey Unit Gypsum- Bearing Clay
	Top	Middle	Bottom	Sand	Top	Middle	Bottom	Top	Middle	Bottom	
	Clay	Clay	Clay		Sandy Clay	Sandy Clay	Sandy Clay	Clay	Clay	Clay	
Ca/Mg	0.197	0.198	0.332	0.292	0.805	0.767	0.129	0.825	0.182	0.340	0.345
Ca/Al	0.063	0.063	0.061	9.056	0.052	0.022	0.072	0.042	0.054	0.062	0.118
Mg/Al	0.320	0.315	0.184	0.193	0.065	0.028	0.548	0.051	0.297	0.183	0.342
Na/Al	0.101	0.073	0.077	0.083	0.106	0.050	0.072	0.127	0.090	0.090	0.107
K/Al	0.151	0.176	0.185	0.199	0.323	0.151	0.165	0.241	0.165	0.165	0.168
Fe/Al	0.200	0.183	0.181	0.233	0.134	0.170	0.191	0.140	0.158	0.165	0.184
Ti/Al	0.022	0.020	0.024	0.020	0.023	0.006	0.029	0.022	0.021	0.022	0.029
Al, M/kg	3.05	2.85	2.54	2.36	1.27	3.05	2.62	1.58	2.72	2.72	2.51
Cu, ppm	26.2				18.8			26.2			
Zn, ppm	132				80			110			
Pb, ppm	< 0.2				< 0.2			< 0.2			
Ni, ppm	< 0.2				< 0.2			< 0.2			
Cr, ppm	124				60			72			
Mn, ppm	221				228			211			
Li, ppm	96				51			82			

Depth intervals of top, middle, bottom, clast, and grey unit are given in Figure 3.

chemical analyses. It is possible that the 6Z hard grey unit is the same stratigraphic unit as the hard grey unit in 6T. Minor amounts of gypsum were observed in the clay unit overlying the hard grey unit in core 6T but not in 6Z. It is unclear whether minor gypsum in the 6T clay unit is primary, secondary, or a phase formed by precipitation from pore fluids as samples dried during storage in the laboratory.

Clay minerals make up 22% of the bulk sediment in core 7B, 68% in core 7A, 20% in core 6Z, and 45% in core 6T. The mineralogical composition of the clay size fraction in all four cores is dominated by smectite. Based on observation of the (060) reflection, the smectite present in all four cores is trioctahedral. There is no consistent correlation between percent clay in the bulk sediment and mineralogical or chemical composition of the clay size fraction. Minor amounts of quartz and calcite are present even in the <2 μm fraction.

Evidence for thermally enhanced diagenesis can be seen by comparing the relative proportion of

calcite to dolomite and smectite to illite plus kaolinite in the lower-temperature cores versus the higher-temperature cores. The relative proportion of calcite to dolomite in the bulk sediment decreases from cores 6T and 6Z toward 7B and 7A. The relative proportion of smectite to illite plus kaolinite in the clay size fraction increases from cores 6T and 6Z toward 7B and 7A. This suggests that more rapid dolomitization of calcite and clay mineral recrystallization is occurring in response to increased temperatures in the interior of the thermal anomaly, in the vicinity of wells 7B and 7A, than at the edge of the thermal anomaly near wells 6T and 6Z.

Bulk Sediments Chemical Composition

The bulk sediment major element molar ratios data do not show clear trends attributable to hydrothermal reactions, with the exception of Ca/Al and Mg/Al, and therefore Ca/Mg, molar ratios. Both Ca/Al and Mg/Al ratios show increases from wells 6T and 6Z toward wells 7B

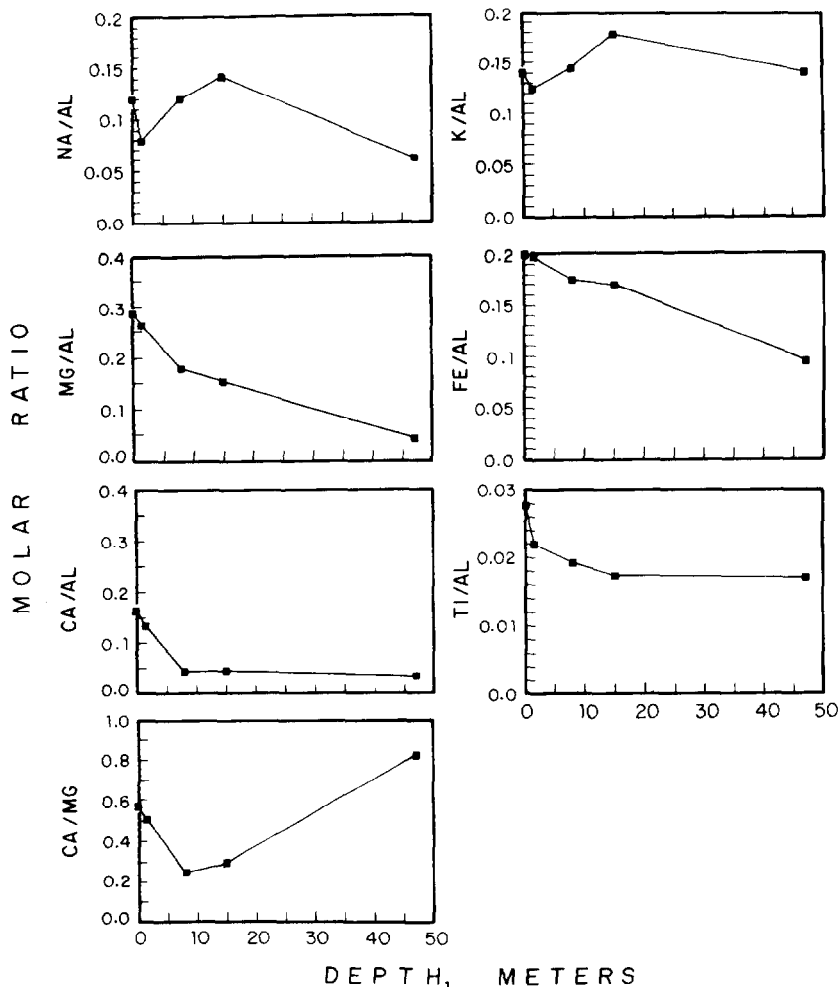


Fig. 5. Bulk chemical composition of cuttings, molar ratio versus depth (in meters) in well 7B.

and 7A. Mg/Al increases at a greater rate than Ca/Al; therefore Ca/Mg decreases from well 6T toward 7B. This trend may reflect the observed increase in dolomite relative to calcite from wells 6T and 6Z toward 7B and 7A or a decrease in calcite abundance only or the uptake of magnesium by clay minerals. Except for copper and manganese, trace and minor elements show the highest relative concentrations in well 7A.

Cuttings from a high-temperature well, 7B, were analyzed at five downwell intervals. Salton Sea water was used as the lubricant during drilling. Because Salton Sea sediments are relatively unconsolidated, this procedure eliminated the fine grain size fraction from the cuttings recovered. Notwithstanding, general downhole chemical trends are observed (Figure 5). Mg/Al molar ratio decreases with depth. Ca/Al and Ti/Al molar ratios decrease in the upper 10 to 15 m of sediment but do not decrease further with depth down section. Na/Al and K/Al molar ratios decrease in the upper 2 m, increase to about 15 m depth, then decrease toward the 45 m depth interval. Fe/Al molar ratio decreases with depth. Because these data reflect the chemical composition of the coarse size fraction, they may reflect downhole variation in bulk sediment chemical composition that is controlled by the original detrital assemblage. However, if these

geochemical trends would be attributed to hydrothermal alteration, they can be interpreted as thermally accelerated exchange reactions which result in leaching of titanium, iron, and potassium with depth and increasing temperature.

At relatively low temperatures of alteration, where reactions proceed more slowly and with less intensity than at the temperatures observed within the geothermal reservoir, the geochemical overprint produced by hydrothermal activity is expected to be small. The bulk sediment chemical composition, and especially the coarse size fraction chemical composition, would be dominated by the original detrital assemblage. Here, the chemistry and mineralogy of the authigenic precipitates are more indicative of the geochemical system. The most commonly observed secondary minerals, both in field and in experimental studies, are clay minerals [e.g., Bass, 1976; Honnorez et al., 1983; Haymon and Kastner, 1986; Mottl and Seyfried, 1980; Thornton and Seyfried, 1987]. Therefore the analyses of the clay fraction of the sediments was emphasized in this study.

Clay Size Fraction Chemical Composition

The chemical compositions of the clay size solids confirm the observation from the pore

TABLE 3. Chemical Compositions of the Sediments Clay Size Fraction

Molar Ratio	7B Top	7A Top	6T Middle	6Z Middle	Percent Error
Ca/Mg	0.014	0.019	0.021	0.023	
Ca/Al	0.003	0.004	0.005	0.005	
Mg/Al	0.210	0.227	0.238	0.222	
Na/Al	0.046	0.086	0.099	0.058	
K/Al	0.184	0.175	0.173	0.176	
Fe/Al	0.214	0.239	0.250	0.201	
Ti/Al	0.023	0.028	0.023	0.025	
Al ₂ O ₃	18.7	18.2	15.9	18.6	3
CaO	6.17	8.97	8.97	11.22	5
MgO	3.12	3.29	2.99	3.56	2
Na ₂ O	0.53	0.96	0.96	0.65	2
K ₂ O	3.20	2.97	2.54	3.02	4
Fe ₂ O ₃	6.31	6.87	6.23	5.83	6
TiO	0.67	0.80	0.58	0.71	4
Cu	48.3	35.6	37.3	33.6	1
Zn	194	191	191	188	3
Pb*					
Ni	123	114	114	78	1
Cr	183	163	163	131	8
Mn	471	437	422	337	1
Li	119	136	104	136	1

Element/Al are in molar ratios. Oxides are in weight percent. Trace element concentrations are in ppm. Depth intervals of top and middle are given in Figure 3.

*All less than 0.2.

water chemical trends that hydrothermal reactions are occurring with increasing intensity along a transect from wells 6T and 6Z toward well 7B. This trend is seen most clearly in the Ca/Al, Mg/Al, Ca/Mg, and K/Al molar ratios (Figure 6). Increasing concentrations of calcium, magnesium, and potassium in the clay size fraction may indicate clay recrystallization and possibly dolomitization of calcite. The differences between clay size fraction metals concentrations for wells 7A, 7B, 6T, and 6Z are very close to the error limits for these analyses. Therefore these data are difficult to interpret. However, if these data are taken at face value, they conform with the bulk sediment chemical composition and pore water data. The highest concentrations of copper, zinc, nickel, chromium, and manganese are found in core 7B, the hottest of the wells which show a linear thermal profile.

When compared to the chemical composition data for wells 7B, 6Z, and 6T, the clay size fraction data for well 7A are anomalous. Core 7A has the highest relative proportion of clay minerals. The anomalous clay chemical composition may be a reflection of original depositional chemical differences between primary minerals. Greater proportion of detrital clay minerals would provide relatively low primary permeability. Low permeability may, in turn, retard hydrothermal exchange by restricting fluid flow. However, the relatively high (90°C) bottom-hole temperature, the nonlinear character of the thermal profile in well 7A and the nearby fumaroles are evidence for hydrothermal alteration in the presence of fluid flow. If the geochemical signature recorded in the clay size solids from core 7A is considered to be a result of hydrothermal alteration, this

is further evidence for anomalous thermal and chemical activity in the region of well 7A. Ca/Mg molar ratio is higher and K/Al is lower than predicted by the chemical trends observed in the other wells. Based on the bottom-hole temperature data observed in well 7A, one would expect to see relatively more advanced hydrothermal alteration, hence lower Ca/Mg and higher K/Al in the clay size fraction. This is more in accordance with the chemical concentrations observed in well 7B. If, however, the area near well 7A is experiencing anomalous fluid flow, the hydrothermal alteration could reflect a distinct fluid chemical composition, as indeed observed. Shallow lateral fluid flow may allow mixing of in situ pore fluids with Salton Sea water. Concentrations of calcium, potassium, lithium, and base metals in such a mixed fluid would be relatively low compared to the unmixed pore fluid. Silica is relatively high in Salton Sea water but is lower in the pore fluids for wells 6T, 6Z, and 7A. One would expect to see higher concentration of silica in 7A pore fluid if mixing with Salton Sea water has occurred. However, clay recrystallization may withdraw silica from the pore fluid at a greater rate than it can be renewed by mixing with Salton Sea water. Clay minerals which form in the presence of such a distinct fluid might also have a distinct chemical composition.

Pore water chemical compositions are very sensitive indicators of hydrothermal activity. Therefore changes in pore water chemical composition can occur quite rapidly. However, secondary solids are less sensitive to changes in environment. They require that alteration occur over a longer period of time in order for changes

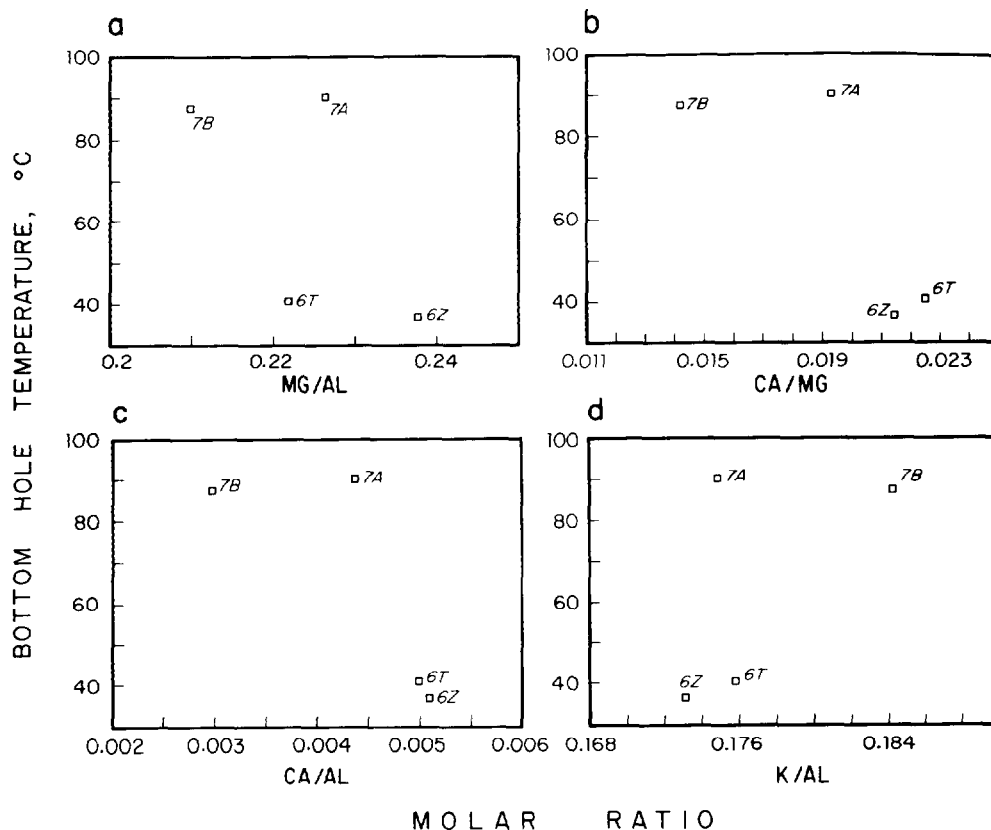


Fig. 6. Chemical composition of clay size fraction of sediment as molar ratios versus bottom-hole temperature (in degrees Celsius): (a) Mg/Al, (b) Ca/Mg, (c) Ca/Al, (d) K/Al.

in chemical composition of secondary solids to be detectable. The chemical composition of the clay size fraction as well as of the pore water in well 7A are anomalous when compared to the other three wells, suggesting that the cause of this anomaly is relatively long lived.

Conclusions

The Salton Sea Geothermal Area is a well-documented region of hydrothermal alteration at a sediment-blanketed oceanic spreading axis. A magma intrusion provides a source of heat which has altered sediments at depths greater than 500 m and at temperatures in excess of 300°C. Near-surface sediments overlying the deep-seated thermal reservoir are exposed to much lower temperatures. Hydrothermally accelerated reactions between pore fluid and solid phases occur at burial depths of less than 100 m at temperatures less than 100°C. These rather low-temperature reactions have altered the chemical composition of the pore fluid and to a lesser degree the mineralogical and chemical composition of the sediment. Calcium, silica, potassium, lithium, and strontium are being released into the fluid phase. The observed thermally accelerated recrystallization of clay minerals and dolomitization are geochemical processes which occur in near-surface sediments in response to increased geothermal gradients. They may contribute to permeability reduction enhancing the original depositional permeability of the

lacustrine sediments of interbedded shale units with sand. The original permeability could be decreased by sealing tectonically formed microfractures and by secondary mineral precipitation in pore spaces within the more permeable layers.

The nonlinear temperature gradient in well 7A may indicate thermal leakage and localized fluid flow in the otherwise uniform thermal regime of this region. In fact, Newmark et al. [1988] observe several such very small scale thermal perturbations within the region of their Shallow Thermal Gradient study (R. Newmark, personal communication, 1987). The data acquired in this study do not support chemical reactions between the deep-seated reservoir brine and the surface sediments in the vicinity of well 7A; these data do, however, suggest shallow depth fluid flow in the vicinity of this well.

Acknowledgments. I acknowledge financial support from Scripps Institution of Oceanography and Lawrence Livermore National Laboratories (IGPP-LLNL 87-13). I would like to thank Miriam Kastner, Scripps Institution of Oceanography, for advice and encouragement throughout this project. I would, also, like to thank T. E. C. Keith and S. D. McDowell for helpful manuscript reviews.

References

Bass, M.N., Secondary minerals in oceanic basalt, with special reference to leg 34, Deep Sea

- Drilling Project, Initial Rep. Deep Sea Drill. Proj., 34, 393-437, 1976.
- Bischoff, J.L., and F.W. Dickson, Seawater-basalt interaction at 200°C and 500 bars: Implications for origin of seafloor heavy metal deposits and regulation of seawater chemistry, Earth Planet. Sci. Lett., 25, 385-397, 1975.
- Bischoff, J.L., and W.E. Seyfried, Hydrothermal chemistry of seawater from 25°C to 350°C, Am. J. Sci., 278, 838-860, 1978.
- Brown, T., Wet chemical analysis of marine sediments: Applications to hydrothermal sediments of Guaymas Basin, Master's thesis, San Diego State Univ., San Diego, Calif., 1988.
- Elders, W. E., Notes on geology, geothermics and ore genesis in the Salton Trough, Soc. Econ. Geologists Field Trip, Feb. 24-26th, Rep. UCR/IGPP 85/4, pp. 1-37, Inst. of Geophys. and Planet. Phys., Univ. of Calif., Riverside, 1984.
- Gieskes, J.M., Interstitial water studies, Leg 15 -alkalinity, pH, Mg, Ca, Si, PO₄, and NH₄, Initial Rep. Deep Sea Drill. Proj., 20, 813-829, 1973.
- Gieskes, J.M., The chemistry of interstitial waters of deep sea sediments: Interpretation of Deep Sea Drilling data, in Chemical Oceanography, vol. 8, edited by J.P. Riley and R. Chester, pp. 221-269, Academic Press, New York, 1983.
- Gieskes, J.M., A.C. Campbell, T. Shaw, T. Brown, and A. Sturz, Interstitial water and hydrothermal water chemistry, Guaymas Basin, Gulf of California, Mem. Am. Assoc. Pet. Geol., in press, 1989.
- Haymon, R.M., and M. Kastner, The formation of high temperature clay minerals from basalt alteration during hydrothermal discharge on the East Pacific Rise axis, 21°N, Geochim. Cosmochim. Acta, 50, 1933-1939, 1986.
- Helgeson, H.C., Geological and thermodynamic characteristics of the Salton Sea geothermal system, Am. J. Sci., 266, 129-166, 1968.
- Honnorez, J., A.-M. Karpoff, and D. Trauth-Badaut, Sedimentology, mineralogy and geochemistry of green clay samples from the Galapagos hydrothermal mounds, Holes 506, 506C and 507D, Deep Sea Drilling Project leg 70 (preliminary data), Initial Rep. Deep Sea Drill. Proj., 70, 211-224, 1983.
- Mottl, M.J., and W.E. Seyfried, Subseafloor hydrothermal systems: Rock- vs seawater-dominated, in Seafloor Spreading Centers: Hydrothermal Systems, edited by P.A. Rona and R.P. Lowell, pp. 66-82, Dowden, Hutchinson and Ross, Inc., Stroudsburg, Pennsylvania, 1980.
- Muffler, J.L.P., and B.R. Doe, Composition and mean age of detritus of the Colorado River delta in the Salton Trough, southern California, J. Sediment. Petrol., 38, 384-399, 1968.
- Muffler, J.L.P., and D.E. White, Active metamorphism of upper Cenozoic sediments in the Salton Sea Geothermal Field and the Salton Trough, southern California, Geol. Soc. Am. Bull., 80, 157-182, 1969.
- Newmark, R.L., P.W. Kasameyer, L.W. Younker, and P.C. Lysne, Research drilling at the Salton Sea Geothermal Field, California: The Shallow Thermal Gradient Project, Eos Trans. AGU, 67, 689-707, 1986.
- Newmark, R.L., P.W. Kasameyer, and L.W. Younker, Shallow drilling in the Salton Sea region: The thermal anomaly, J. Geophys. Res., 93, 13005-13023, 1988.
- Randall, W., An analysis of the subsurface structure and stratigraphy of the Salton Sea geothermal anomaly, Imperial Valley, California, Ph.D. thesis, Univ. of Calif., Riverside, 1974.
- Rex, R.W., The origin of the brines of the Imperial Valley, California, Trans. Geotherm. Resour. Council, 7, 321-324, 1983.
- Skinner, B.J., D.E. White, H.J. Rose, and R.E. Mays, Sulfides associated with the Salton Sea geothermal brine, Econ. Geol., 62, 316-330, 1967.
- Stout, P.M., and A.C. Campbell, Hydrothermal alteration of near surface sediments, Guaymas Basin, Gulf of California, in Cenozoic marine sedimentation, Pacific Margin, USA, edited by D.K. Larue and R.J. Steel, pp. 223-231, Pacific Section, Society of Economic Paleontologists and Mineralogists, Bakersfield, Calif., 1983.
- Thornton, E.C., and W.E. Seyfried, Reactivity of organic-rich sediment in seawater at 350°C, 500 bars: Experimental and theoretical constraints and implications for the Guaymas Basin hydrothermal system, Geochim. Cosmochim. Acta, 51, 1997-2012, 1987.
- Von Damm, K.L., J.M. Edmond, C.I. Measures, and B. Grant, Chemistry of submarine hydrothermal solutions at Guaymas Basin, Gulf of California, Geochim. Cosmochim. Acta, 49, 2221-2237, 1985.
- Younker, L.W., P.W. Kasameyer, and J.D. Tewey, Geological, geophysical and thermal characteristics of the Salton Sea Geothermal Field, California, J. Volcanol. Geotherm. Res., 12, 221-258, 1982.

A. Sturz, Scripps Institution of Oceanography, Geological Research Division, University of California, San Diego, La Jolla, CA 92093.

(Received June 7, 1988;
revised November 16, 1988;
accepted November 21, 1988.)